Sensors & Actuators: B. Chemical 335 (2021) 129688

Contents lists available at ScienceDirect

Sensors and Actuators: B. Chemical

journal homepage: www.elsevier.com/locate/snb

Monitoring of the evolution of human chronic wounds using a ninhydrin-based sensory polymer and a smartphone

Marta Guembe-García [a], Victoria Santaolalla-García [b], Natalia Moradillo-Renuncio [b], Saturnino Ibeas [a], Jose A. Reglero [a], Félix C. García [a], Joaquín Pacheco [c], Silvia Casado [c], José M. García [a,*], Saul Vallejos [a,*]

[a] Departamento de Química, Facultad de Ciencias, Universidad de Burgos, Plaza de Misael Bañuelos s/n, 09001, Burgos, Spain
[b] Complejo Asistencial Universitario de Burgos, Avenida de las Islas Baleares, 3, 09006, Burgos, Spain
[c] Departamento de Economía Aplicada, Facultad de C. Económicas y Empresariales, Universidad de Burgos, Calle Parralillos, s/n, 09001, Burgos, Spain

ARTICLE INFO

Keywords:
Monitoring human chronic wounds
Polymer chemosensor
Smartphone

ABSTRACT

The healing processes in cutaneous wounds, i.e., chronic wounds, represent a health problem affecting 1–2 % of the population. The evaluation of these wounds is mainly based on subjective parameters, although there is a medical consensus on protease activity as the best marker for healing disorders. Here we show the correlation of the amino acid concentration on chronic wounds and with their evolution, and the development of a test kit to straightforward determining this evolution. Our test kit is a colorimetric sensory polymer film that change its colour upon contacting amino acids. The kit allows for the quantification of the overall amino acid concentration by simply analysing the colour definition parameters of the sensory film obtained from of a photograph taken with a smartphone. We analysed with the kit the amino acid concentration of human chronic wounds of 34 patients and we mathematically demonstrate that there is a correlation with the amino acid concentration, related with the protease activity, and the evolution of the wound's diagnoses. This kit can help diagnosis of human chronic wounds, usually evaluated and treated along time by different physicians, or even by different medical teams, providing an analytical tool not subjected to subjective evaluation.

1. Introduction

Nowadays, the medical researches related to the cure for cancer, or the development of new vaccines against viruses, such as HIV or coronavirus, are very current issues. But there are other health problems that a priori may seem milder but have a significant impact on society, both due to the large number of people who are affected by them and the economic costs they cause. In this work, we will focus on one of these well-known health problems [1,2], with high impact [3–7], and little visibility: the healing processes in cutaneous wounds, that is, chronic wounds. These types of low visibility injuries (affecting 1–2 % of the population) represent 2–3 % of the total European health budget [8]. According to estimates, in Europe, these wounds signify costs of 2.8–3.5 million euros per 100,000 habitants. Nurses dedicate the equivalent of 89 days to cures, and it is estimated that patients with these conditions occupy 19,000–31,000 bed days per year [9]. In the USA, the economic impact of chronic injuries has been estimated at 32,000 million dollars per year [10], and only in Spain 350 million € per year [8].

This type of wounds requires weekly monitoring (even daily, in case of hospitalised patients). This follow-up is carried out by a physicians through a form where the state of the wound is assessed, regarding factors such as the appearance of infection (Y/N), revascularisation (Y/N), date of revascularisation, evolution, necrosis (Y/N), ischemia (Y/N) or cell cultures performed (*Pseudomonas aeruginosa, Proteus mirabilis, Staphylococcus aureus, Prevotella bivia, Enterococcus faecalis, Escherichia coli*). The problem with these evaluations is that many of the parameters are subjective. Additionally, due to the shifts and schedules of the health workers, throughout the same week, a patient can be attended by 2 or 3 different physicians, with varying opinions about the state of the wound, which generates a high variability on the results. At this point, the need for a methodology based on a simple kit becomes evident, which physicians can use to objectively determine the state/evolution of the wounds.

Although nowadays there are currently not clear solutions to this

* Corresponding authors.
E-mail addresses: jmiguel@ubu.es (J.M. García), svallejos@ubu.es (S. Vallejos).

https://doi.org/10.1016/j.snb.2021.129688
Received 3 November 2020; Received in revised form 2 February 2021; Accepted 17 February 2021
Available online 26 February 2021

problem, there is a medical consensus among the World Union of Wound Healing Societies [11], "that increased protease activity is currently the best available marker for healing disorders when other causes have been excluded, and that the effective use of a protease test kit has the potential to change wound management globally" [12,13]. Proteases are the enzymes responsible for the degradation into peptides and amino acids of proteins. They are believed to play a crucial role in healing processes as they degrade damaged extracellular matrix (EM) proteins, thereby allowing new tissue formation in an orderly healing process. Healing problems appear when the degradation/regeneration balance is altered, due to the uncontrolled activity of the protease that not only breaks the damaged EM proteins but also degrades the newly formed EM and other essential EM proteins, like growth factors and their receptors. This uncontrolled degradation prolongs the inflammatory phase preventing the wound to progress to the proliferative phase.

Thus, determining the enzymatic activity of a wound seems to be the key to diagnosing this type of lesions at an early stage, since at first sight, they are not easy to detect in their early stages because clinical signs of inflammation are usually challenging to discriminate from the signs of infection. This is an important issue since there is currently no fast and reliable method for evaluating enzyme activity. Techniques such as gelatine zymography [14,15], and the Enzyme-Linked Immunosorbent Assay (ELISA) [16], determines protease levels using antibodies but, in most cases, they are beyond the reach of physicians.

Since proteases hydrolyse ME proteins, we hypothesise that the higher the enzyme activity, the higher the amino acid concentration. This hypothesis would allow us to address the problem indirectly by measuring the concentration of amino acids derived from enzyme activity and not the activity directly. Within the literature, the detection of amino acids is an intensely studied subject and for which there are several techniques such as electrophoresis [17,18], HPLC [19,20], NMR [21], or chromatography [22–24]. However, all of these methods require expensive equipment and advanced knowledge for amino acid detection.

One of the oldest and most studied methods [25,26] is that of ninhydrin [27–30], a colorimetric method widely used in forensic science [25,31,32]. However, this method implies both the manipulation of chemicals and the use of relatively costly equipment, which undoubtedly complicates their daily use in hospitals and/or health centres. Gel behaviour polymers have been widely used for sensory applications oriented to different areas [33–36], and for this reason, we propose a sensory film, with gel behaviour, simple, cheap and easy to use by non-specialized personnel, based on ninhydrin receptors but without the need to manipulate any chemical reagent, which determines enzymatic activity in the wounds indirectly, by measuring the amino acid concentration of exudates from a skin wound through a digital photo taken with a smartphone.

This work is focused in two correlated objectives. First, the development of a new sensory material for the detection of amino acids in and easy and rapid way, by only using a smartphone. Second, the demonstration that the level of amino acids is directly related to the state of a chronic wound, and subsequently with the protease activity. For the analysis of all this data, the statistical classification methods have boosted the proposed diagnostic tool based on a simple sensory film.

2. Experimental

2.1. Materials

We have used the following materials and solvents, as received, unless otherwise stated: 2,2′-azobis(2-methylpropionitrile) (AIBN) (98 %, Aldrich), 1-vinyl-2-pyrrolidone (**VP**) (99 %, Aldrich), methyl methacrylate (**MMA**) (99 %, Aldrich), pH 4.66 Buffer (VWR), dioxane (100 %, VWR), acetone (99 %, VWR), trans-4-hydroxi-L-proline (≥99 %, Sigma-Aldrich), L-aspartic acid (98 %, Alfa Aesar), L-threonine (98 %, Alfa Aesar), Serine (≥99 %, Fluka), L-arginine (98 %, Alfa Aesar), L-glutamic acid (+99 %, Alfa Aesar), L-lysine (97 %, Sigma-Aldrich), L-proline (99 %, Alfa Aesar), L-histidine (+98 %, Alfa Aesar), Glycine (99 %, Alfa Aesar), L-alanine (99 %, Alfa Aesar), L-cysteine (+98 %, Alfa Aesar), L-valine (≥98 %, Sigma-Aldrich), L-methionine (+98 %, Alfa Aesar), L-isoleucine (98 %, Sigma-Aldrich), L-tyrosine (+99 %, Acros Organic), L-phenylalanine (98 %, Alfa Aesar) zinc (II) nitrate hexahydrate (98 %, Sigma Aldrich), Iron(III) nitrate nonahydrate (99 %, Sigma Aldrich), cesium nitrate (≥99 %, Fluka), manganese (II) nitrate hexahydrate (98+%, Alfa Aesar), tetrachloroauric(III) acid trihydrate (99.9+%, Sigma-Aldrich), potassium dichromate (≥99.5 %, Sigma-Aldrich), barium chloride dehydrate (99 %, Labkem), cobalt(II) nitrate hexahydrate (≥99 %, Labkem), ammonium nitrate (≥98 %, Sigma-Aldrich), calcium nitrate tetrahydrate (≥99 %, Sigma-Aldrich), chromium(III) nitrate nonahydrate (98.5 %, Alfa Aesar), mercury(II) nitrate (98 %, Alfa Aesar), rubidium nitrate (99.95 %, Sigma-Aldrich), dysprosium(III) nitrate (99.9 %, Alfa Aesar), lithium chloride (≥ 99 %, Sigma-Aldrich cadmium nitrate tetrahydrate (98.5 %, Alfa Aesar), Fe(NO3)3·9H2O (≥ 98 %, VWR), cerium (III) chloride tetrahydrate (≥99.99 %, Sigma-Aldrich), zirconium(IV) chloride (98 %, Alfa Aesar), lanthanum(III) nitrate hexahydrate (99.9 %, Alfa Aesar), potassium nitrate (99+%, Sigma-Aldrich), samarium(III) nitrate (99.9 %, Alfa Aesar), magnesium nitrate hexahydrate (≥ 99 %, Labkem), aluminum nitrate nonahydrate (≥ 98.9 %, Sigma-Aldrich), silver nitrate (≥99.9, Sigma-Aldrich), neodymium(III) nitrate (99.9 %, Alfa Aesar), lead(II) nitrate (≥ 99 %, Fluka), strontium nitrate (99+%, Sigma-Aldrich), copper(II) nitrate trihydrate (98 %, Sigma-Aldrich), nickel(II) nitrate hexahydrate (98.5 %, Sigma-Aldrich), sodium nitrate (99 %, LabKem), tin (II) chloride (98 %Aldrich), Sodium cyanide (>97 %, Sigma-Aldrich), Sodium acetate (>99 %, Aldrich), Lithium hydroxide (>98 %, Sigma-Aldrich), Sodium fluoride (≥99.9 %, Sigma-Aldrich), Potassium perchlorate (>99 %, Sigma-Aldrich), Sodium dodecyl sulfate (≥98.5 %, Sigma-Aldrich), Sodium nitrite (>97 %, Aldrich), Sodium Ethoxide (95 %, Sigma-Aldrich), Potassium hydrogen phthalate (99.95 %, Sigma-Aldrich), Sodium pyrophosphate tetrabasic (>95 %, Sigma-Aldrich), Potassium persulfate (>99 %, Sigma-Aldrich), Sodium methanesulfonate (98 %, Sigma-Aldrich), Sodium pyrophosphate dibasic (>99 %, Sigma-Aldrich), Lithium trifluoromethanesulfonate (96 %, Sigma-Aldrich), Sodium *p*-toluenesulfonate (95 %, Sigma-Aldrich), Potassium bromide (>99 %, Sigma-Aldrich), Potassium thiocyanate (>99 %, Sigma-Aldrich), Potassium oxalate monohydrate (>98.5 %, Sigma-Aldrich), Sodium carbonate (>99 %, Sigma-Aldrich), Sodium benzoate (>99.5 %, Sigma-Aldrich), Lithium phosphate monobasic (99 %, Sigma-Aldrich,), Sodium sulfate (99 %, Sigma-Aldrich), Sodium chloroacetate (98 %, Sigma-Aldrich), Sodium trifluoroacetate (>99 %, Sigma-Aldrich), Sodium periodate (99.78 %, Sigma-Aldrich, 99.8 %), bovine serum albumin (BSA) (>97 %, Biowest), L-Glutathione reduced (GLUT) (VWR, >98 %), SeO_2 (99.4 %, Alfa Aesar), HCl(37 %, VWR-Prolabo), sodium dodecyl sulfate (≥97 %, Fluka), di-sodium tetraborate (99 %, Sigma-Aldrich), phthaldialdehyde (97 %, Merk), 2-mercaptoethanol (98+%, Alfa Aesar), Selenium dioxide (98 %, Fluka, Caution, toxic!).

We have prepared three solutions mimicking collagen (**COL**), elastin (**ELA**) and epidermis (**EPI**), following the procedure described in a previous work [37], by mixing different concentrations of the amino acids which these proteins are constituted of, as reported by Eastoe [38], Keeley and Partrige [39], and Eastoe et al. [40]. The concentration of **COL**, **ELA** and **EPI** are expressed as the summation of the molarities of each amino acid (ΣM).

Food matrix, beef, loin cut, was used to test the polymer described in this work as amino acid sensor. For it, the results of the proposed method in this work were compared with the results of the Nielsen method (reference method for the amino acids detection) [41]. The food matrix was purchased from a local supermarket (see **ESI section S6, Figure S10**).

The real biological samples (exudates) from patients with chronic wounds have been obtained following the established procedures at HUBU (University Hospital of Burgos), directly from the damaged tissue.

Thus, tissue sample collection was carried out with validated aseptic technique after mechanical dragging with physiological saline of any drug residue or detritus. In cases where there is dry crust or abundant accumulation of devitalized tissue, they are actively removed with a scalpel until a representative bed of the ulcer is obtained. The samples are two-ways collected: 1) by means of a bottom swab smear of the lesion; 2) by physical debridement with a scalpel in the different areas of loss of substance depending on the anatomical location of the lesion and its extension in surface and depth (edges, bottom, bone, tendon, etc.), obtaining a piece of vital tissue of the size to proceed according to the condition of the wound. The sample is deposited in a suitable means of transport that allows the correct later analysis. The study was carried out with five types of samples of a chronic wounds of each patient, and picked up from 35 patients: swab (A), wound bed (B), edge (C), capsular tissue (D) and/or bone (E). Samples were collected by physicians who previously performed a visual analysis of the wounds, evaluating also other factors such as age, type of sample (A, B, C, D, E), re-vascularised date, site injury, infectious appearance (Y/N), bad evolution (Y/N), necrosis (Y/N), ischemia (Y/N) and cell cultures (*Pseudomonas aeruginosa, Proteus mirabilis, Staphylococcus aureus, Prevotella bivia, Enterococcus faecalis, Escherichia coli*) and note about evolution. We understand by *bad evolution* of a wound if there are criteria of infection or lack of healing in a given period. Signs of infection are pain, heat, perilesional erythema, bad smell, gas, lymphangitis, crepitus in the area of the injury, and signs of lack of healing are progressive necrosis or reduced granulation tissue at the bottom of the lesion in 4–6 weeks from the appearance of the lesion. All samples were boiled in pH 4.66 buffer solution for 10 min (20 mL of pH 4.66 buffer solution per gram of sample). Finally, samples were filtered at room temperature, and the resulting solutions were labelled as **CWS** (chronic wound samples).

2.2. Measurements and instrumentation

The method for measuring amino acid concentrations with pictures taken to sensory films (from now on RGB_method) was carried out by taking digital photography of the sensory discs (8 mm diameter) with an iPhone 6S smartphone after immersion in a mixture of 1:1 buffer pH = 4,66: aqueous solutions with different concentrations of amino acids at 100 °C for 1 h. The pictures were made in a homemade retro-illumination box, manufactured with 3D printing, to obtain a good reproducibility of the results, as well as to avoid possible external influences in the photographs (for practical purposes, the influence of ambient light and digital camera could be disregarded using a colour reference, [42,43]). The digital pictures were analysed with a generic image software to obtain the R (red), G (green) and B (blue) parameters (RGB) of the entire surface of the sensory disc. Photos were made six-fold for the calculations of the errors, and the average of each RGB parameter was calculated. This easy and cheap method allows the quantification of amino acid in aqueous media, by only taking a photo, and we have widely used it in previous works [44,45].

Principal component analysis (PCA) was carried out using the Statgraphics Centurion XVI software installed on a personal computer in a Windows 7 environment. The principal component (**PC**) values were obtained from RGB parameters, carrying out a multivariate analysis of principal component. This mathematical method allows the simplification of 3 variables to a single one [46], transforming a colour in a number. Values were standardised and accounted for >99 % of the variance in all experiments.

Infrared spectra (FTIR) were recorded with an FT/IR-4200 FT-IR Jasco Spectrometer with an ATR-PRO410-S single reflection accessory. ^{1}H and $^{13}C\{^{1}H\}$ NMR spectra were recorded with a Bruker Avance III HD spectrometer operating at 300 MHz for ^{1}H, and 75 MHz for ^{13}C, using deuterated solvents like dimethyl sulfoxide (DMSO-d_6) or deuterated chloroform ($CDCl_3$) at 25 °C. Solid-state ^{13}C CPMAS NMR spectra were recorded on a Bruker AVANCE III, 9.4 T system equipped with a 4 mm MAS DVT Double Resonance HX MAS probe. Larmor frequencies were 400.17 MHz and 100.63 MHz for ^{1}H and ^{13}C nuclei, respectively. Chemical shifts were calibrated indirectly with glycine, carbonyl peak at 176 ppm. The sample rotation frequency was 10 kHz and the relaxation delay was 5 s. The number of scans were 10240. Polarization transfer was achieved with RAMP cross-polarization (ramp on the proton channel) with a contact time of 5 ms. High-power SPINAL 64 heteronuclear proton decoupling was applied during acquisition.

Thermal and mechanical properties of the material were measured using thermogravimetric analysis (TGA, 10−15 mg of the sample under synthetic air and nitrogen atmosphere with a TA Instruments Q50 TGA analyser at 10 °C min^{-1}), differential scanning calorimetry (DSC, 10−15 mg of the sample under a nitrogen atmosphere with a TA Instruments Q200 DSC analyser at 20 °C min^{-1}), and tensile properties analysis (5 × 9.44 × 0.122 mm samples using a Shimadzu EZ Test Compact Table-Top Universal Tester at 1 mm·min^{-1}). The weight percentage of water taken up by the films upon soaking in pure water at 20 °C until reaching equilibrium (water-swelling percentage, WSP) was obtained from the weight of a dry sample film (ωd) and its water-swelled weight (ωs) using the following expression: $WSP = 100 \times [(\omega s - \omega d)/\omega d]$.

High-resolution electron-impact mass spectrometry (EI-HRMS) was carried out on a Micromass AutoSpect Waters mass spectrometer (ionisation energy: 70 eV; mass resolving power: >10,000).

UV/Vis spectra were recorded using a Hitachi U-3900 UV/Vis spectrophotometer.

RAMAN spectra were recorded with a confocal AFM-RAMAN model Alpha300R – Alpha300A AFM from WITec, using a laser radiation of 532 nm, at magnifications of 100 × . All spectra were taken at room temperature.

Chronic wounds were initially visually analysed by physicians. Then, all **CWS** were analysed by two methods: reference method based on Nielsen's method (see **ESI section S6)** and RGB_method explaining in this work [41]. All data obtained were analysed by statistical linear and non-linear methods for diagnosis and classification, such as Discriminant Analysis (**DA**) [47], Logistic Regression (**LR**) [48], or Support Vector Machine (**SVM**) [49–51].

2.3. Monomer synthesis

For the synthesis of a polymer with ninhydrin-based receptor units, the synthesis of a monomer with a reactive side moiety was performed following the same philosophy as in previous works [45,52,53]. Instead of carrying out the complete synthesis of the sensory monomer, we prepared a monomer which subsequent free-radical-initiated polymerization in bulk rendered a functional polymer film that was transformed into the sensory polymer containing ninhydrin-based receptors by straightforward solid phase synthesis. Compared to conventional monomer synthesis, this methodology is cost effective and greener, it reduces both the use of solvents and the time needed.

The preparation and characterization of the monomer with the reactive side moiety, which is a derivative of 6-aminoindanone, is described in the electronic supplementary information**, ESI section S1,** and shown schematically in Scheme 1.

2.4. Polymer synthesis

2.4.1. Preparation of the sensory film

We obtained the starting material by thermally initiated radical copolymerisation of two main co-monomers, one hydrophilic (vinylpyrrolidone, **VP**) and the other hydrophobic (methylmethacrylate, **MMA**), and the monomer with the reactive side moiety, (**1**). The bulk radical polymerisation was carried out in a silanised glass mould (100 μm thick) in an oxygen-free atmosphere at 60 °C overnight to obtain the membrane $\mathbf{F_1}$. Regarding the molar ratio of the monomers, this can be adjusted for different purposes. In our case, the colorimetric response of the material toward amino acid was modulated by controlling this molar ratio, i.e., 49.5/ 49.5/1 (**VP**/**MMA**/(**1**)). After the bulk radical

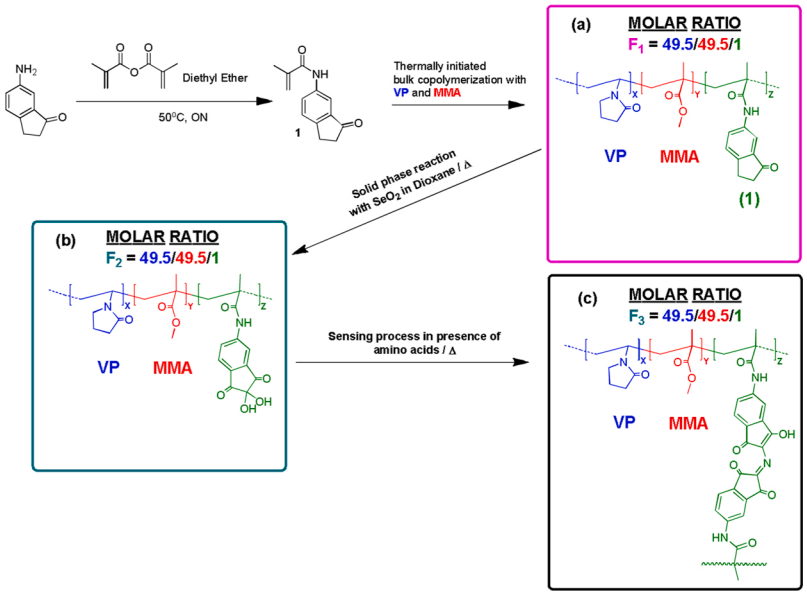

Scheme 1. Synthetic route for the sensory monomer **1** and sensory polymer $\mathbf{F_2}$.

polymerisation, a solid phase reaction was made in the solid membrane to obtain the final sensory material ($\mathbf{F_2}$). We chose solid-phase synthesis to synthesise the anchor monomer derived from ninhydrin because, following the conventional route, the process would require several purifications per column with a high solvent expenditure. Also, this methodology has given us good results in previous works [45,52]. The reaction was carried out as previously depicted for the preparation of different ninhydrin derivates [54]. First, the membranes (4 membranes 13 cm wide and 9 cm long) were washed with 200 mL of dioxane in a pressured flask for one night at RT. Secondly, the dioxane was removed from the flask, and a solution of SeO_2 in dioxane (1 g in 200 mL) was added. The flask was heated at 90 °C for 24 h, or until no colour evolution of the membrane observed in the presence of amino acid. Finally, the solution was removed from the flask, and the films were washed with acetone (2 times) and water (2 times).

The chemical structure of the films used to prepare the sensory materials is depicted in Scheme 1. Additionally, the thermally inititated free.-radical bulk polymerisation procedure for polymers prepared with VP results in crosslinked materials [55], which limits conventional NMR or GPC analysis. Thus, we have developed a sensory film with a higher proportion of ninhydrin units for the characterisation of the materials by FT-IR spectroscopy, Raman spectroscopy and solid-state NMR (see **ESI section S2, Figures S2-S4**).

2.5. Ethical statement

All experiments with human subjects have been performed based on the use and ethics of the HUBU policy for trials with humans. This study (minute 13/2017, internal code: 2017.200, on November 16, 2017) has been approved by the ethics committee of clinical experimentation of the region of Burgos, Spain. According to Spanish Organic Law 15/1999, December 13, related to Spanish Personal Data Protection Regulation and Royal Decree-Law 1720/2007, December 21, all participants of the study were informed and gave their consent.

3. Results and discussion

3.1. Water uptake of films

The water swelling percentage (WSP) was 56 % for $\mathbf{F_1}$, 101 % for $\mathbf{F_2}$ and 38 % for $\mathbf{F_3}$, and envisaged appropriate diffusion of species, such as amino acids, inside the water-swelled sensory film. The increase in swelling between $\mathbf{F_1}$ and $\mathbf{F_2}$ is because the ninhydrin derivative present in $\mathbf{F_2}$ is more hydrophilic than the indanone derivative of $\mathbf{F_1}$. The decrease of the water uptake in $\mathbf{F_3}$ is due to the crosslinking process that results after the reaction of ninhydrin motifs with an amino acid.

3.2. Thermal and mechanical characterisation

An essential property in sensory materials is their manageability. This is related with a good thermal behaviour, with thermal resistance above the higher-expected environmental temperatures, and also with good mechanical properties. Regarding the former, the 5 (T_5) and 10 % (T_{10}) weight loss under nitrogen atmosphere, obtained by TGA, are 360 and 387 °C for $\mathbf{F_1}$, 296 and 355 °C for $\mathbf{F_2}$, and 332 and 370 °C for $\mathbf{F_3}$. The thermal characterization was complemented with the determination of the glass transition temperatures (*Tg*) of the materials DSC. The *Tg* values were 177, 206 and 202 °C for $\mathbf{F_1}$, $\mathbf{F_2}$ and $\mathbf{F_3}$ respectively. The DSC and TGA patterns are shown in the **ESI section S3, Figure S5**. The mechanical properties for $\mathbf{F_1}$, $\mathbf{F_2}$, and $\mathbf{F_3}$ (Young's moduli of 48, 31, and 105 MPa, respectively) were obtained from strips of the water swelled films. These values are very similar for $\mathbf{F_1}$ and $\mathbf{F_2}$, the small differences are due to the swelling in water, in $\mathbf{F_2}$ is higher, so the modulus decreases. In $\mathbf{F_3}$ Young's modulus is higher because of the crosslinking of the material.

3.3. Study of pH

Biological samples usually need specific conditions in terms of pH. Accordingly, we carried out a study of the behaviour of $\mathbf{F_2}$ at different pHs. For it, 14 discs (8 mm diameter) of $\mathbf{F_2}$ were immersed in a mixture of 1 mL of 0.1 M amino acid solution (ΣM) mimicking epidermis (**EPI**), and 1 mL of aqueous solutions with pH ranging from 1 to 14 (HCl: NaOH). The system was heated at 100 °C for 60 min, and the discs were washed with water. Photographs of the discs were taken in the retro-illumination lightbox and were analysed by the RGB_method (**ESI-S4, Table S1**). The results show (Fig. 1) that the sensory material can be used from pH 3–11. In our case, 4.66 was chosen as the working pH.

3.4. Response mechanism and method for measuring amino acid concentrations with photographs taken to sensory films (RGB_method)

The 8 mm discs of $\mathbf{F_2}$ changes their colour upon immersion in water solution of amino acids (pH 4.66) at 100 °C for 60 min. The initial

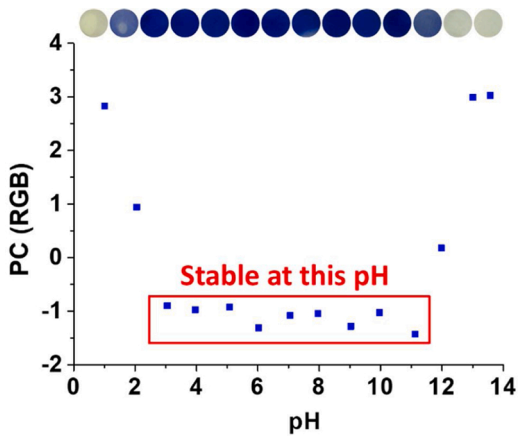

Fig. 1. The pH study was performed using the RGB_method, by immersing 8 mm diameter discs of $\mathbf{F_2}$ in a mixture of 1 mL of 0.1 M **EPI**, and 1 mL of aqueous solutions with pH ranging from 1 to 14 (HCl:NaOH), at 100 °C for 60 min. Then, the discs were washed several times with water, and photographed for the extraction of the RGB variables, which were simplified to a single variable (first principal component, **PC**) through a multivariate analysis. Additional information in **ESI section S4, Table S1.**

orange colour evolves to blue in presence of varying amino acid concentrations (see **ESI-S5, Figure S6)**. The sensing mechanism is depicted in Scheme 1. The sensing mechanism is based on the 'ninhydrin test' in which two molecules of ninhydrin react with a free α-amino acid to render the Ruhemann's purple [56]. Ninhydrin behaves as oxidizing agent causing the deamination and decarboxylation of the amino acids with the concomitant condensation between the reduced ninhydrin residue and the second molecule of ninhydrin with the release of ammonia, giving rise to a highly coloured diketohydrin complex.

In a first stage, we tested our sensory material with amino acid solutions mimicking collagen (**COL**), elastin (**ELA**) and epidermis (**EPI**), as we have depicted in previous works [57]. These are the main proteins conforming the skin, i.e., that are supposed to be related with the protease activity in chronic wounds. Fig. 2 shows the titration of $\mathbf{F_2}$ discs **EPI**, in sum of concentrations of all amino acids ranging from 5×10^{-4} to 1×10^{-2} M (ΣM). Further information related with the fitted curve, and equivalent experiments carried out with **COL** and **ELA** (**ESI-S5, Figure S7-S9**).

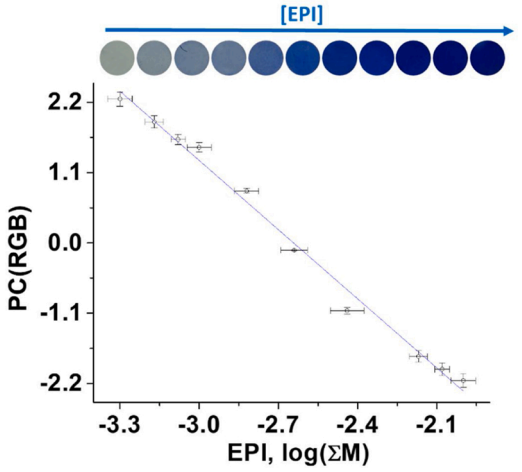

Fig. 2. Titration of $\mathbf{F_2}$ discs with solution mimicking epidermis (**EPI**) was performed with RGB_method. Discs of 8 mm diameter of $\mathbf{F_2}$ were dipped in pH 4.66 buffered solutions of **EPI**, with a sum of concentrations of all amino concentrations ranging from 5×10^{-4} to 1×10^{-2} M (ΣM). After reaction at 100 °C for 60 min, the discs were washed several times with water, and photographed for the extraction of RGB data, which were simplified to a single variable (first principal component, **PC**) through a multivariate analysis. Additional information can in **ESI section S5, Figure S6.**

3.5. Interference study

The study of interferences was carried out with a wide collection of anions and cations (Fig. 3), by immersing an 8 mm diameter disc of $\mathbf{F_2}$ in 1 mL of 4.66 buffer and 1 mL of an aqueous solution of the interferents at high concentration (10^{-2} M), at 100 °C for 60 min. The disc was photographed in the retro-illuminated lightbox. We observed no interferences concerning the application of the sensory material.

3.6. Testing the material with a real sample: food matrix, beef, loin cut

After the test of the sensory material with **COL**, **ELA** and **EPI** solutions, and before the analysis with samples from human chronic wounds, we carried out a proof of concept with a beefsteak from the local market (see **ESI-S6, Figure S10**). The aim of this experiment was the detection of amino acids from the activity of the proteinase papain (papaya proteinase I) on the beefsteak by two different ways, the reference method and RGB_method. The degree of hydrolysis (DH%) produced by papain was measured at different times by reference method, as we explain thoroughly in **ESI section S6**. Additionally, at the same times, $\mathbf{F_2}$ discs were immersed in a mixture of 1 mL from the beefsteak hydrolysis flask and 1 mL of pH 4.66 buffer solution, and the system was heated for 60 min at 100 °C. The discs were washed and photographed for the measurement of the RGB parameters and calculation of the principal component (PC). The results of both methods are shown in Fig. 4, where we can see a good correlation between DH% obtained with the reference method, and PC obtained with RGB_method.

3.7. Analysis of human chronic samples by data mining methods from data obtained with our methodology (RGB_method)

Once checked the response of the sensory discs to amino acids in the lab-prepared solutions (**COL**, **ELA** and **EPI**), and after the successful proof of concept following the proteinase activity of papain on a beef steak, we decided to initiate a study with 34 patients (all data can be found in **ESI section S7, Table S12)**. The main objectives of this work are two: **1**) to replace the reference method used so far for the quantification of amino acids, by the method that we propose in this work based on our sensory materials; **2**) to demonstrate that the amino acid concentration of a chronic wound is directly correlated with the state of the wound (according to the visual analysis of the medical personnel). For both, we have analysed five types of samples from each chronic human wound: swab (A), wound bed (B), edge (C), capsular tissue (D) and/or bone (E). Physicians at the HUBU collected the samples, according to the established protocols.

The study was carried out on a representative group of patients, taking into account variables such as age, and wound status. Two questions were stated:

3.7.1. Is there a function f such that reference method = f(RGB_method)?

In this test, we try to establish if there is any kind of functional relationship between the variable obtained from reference method (absorbance at 330 nm, or ABS 330) and the variables R, G, B (which classically determine a colour depending on the values Red, Green and Blue from 0 to 255). The test was performed with a sample of $n = 35$ cases, and three different models have been used: two linear models (Linear Regression, **LinR**, and Support Vector Regression, **SVR**) and a non-linear model (**SVR** with Gaussian Kernel, **SVR-GK**). For each test, we have analysed Mean Square Error (**MSE,** Eq. 1), Mean Absolute Error (**MAE,** Eq. 2) and Fit or $\boldsymbol{R^2}$. Let's be O_i the observed value (each value of ABS 330) and E_i the value estimated for each model, in case i, i = 1…n:

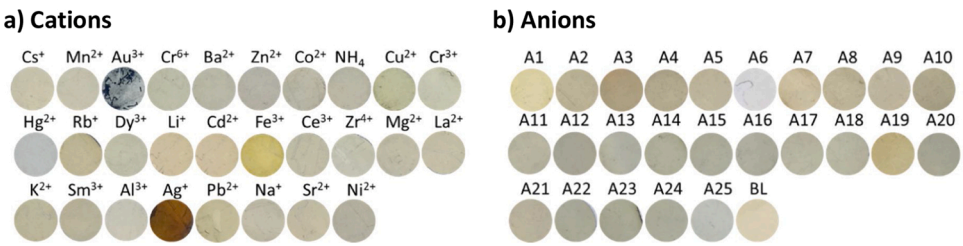

Fig. 3. Discs of $\mathbf{F_2}$ were dipped for 60 min at 100 °C in a mixture of 1 mL of 4.66 buffer and 1 mL of an aqueous solution of the interferents (1×10^{-2} M). a) Cations of nitrate or chloride salt. b) Anions. A1=Cyanide, A2=acetate, A3=hydroxile, A4=fluoride, A5=perchlorate, A6=dodecyl sulfate, A7=nitrite, A8=ethoxide, A9=hydrogen phthalate, A10=pyrophosphate, A11=persulfate, A12=methanesulfonate, A13=pyrophosphate dibasic, A14=trifluoromethanesulfonate, A15=p-toluenesulfonate, A16=bromide, A17=thiocyanate, A18=oxalate, A19=carbonate, A20=benzoate, A21=dihydrogenphosphate, A22=sulfate, A23=chloroacetate, A24=trifluoroacetate, A25=periodate. See materials section.

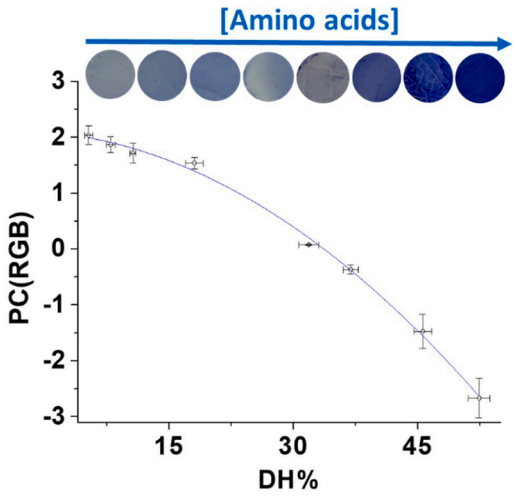

Fig. 4. The figure shows the picture of $\mathbf{F_2}$ discs after dipped for 60 min at 100 °C in a mixture of 1 mL from the beefsteak hydrolysis flask and 1 mL of pH 4.66 buffer solution. After washed with water, the discs were photographed for measuring the RGB parameters and after that calculation of the principal component (firstfirst principal component, PC). The graph shows the correlation of PC with the chosen reference method, which shows the amino acid concentration of the hydrolysis flask, expressed as the degree of hydrolysis (DH %), due to the proteinase activity of the enzyme papain (papaya proteinase I) on the beefsteak. Further information can be found in the **ESI section S6.**

$$MSE = \frac{1}{n}\cdot\left(\sum_{i=1}^{n}(O_i - E_i)^2\right) \quad (1)$$

$$MAE = \frac{1}{n}\cdot\left(\sum_{i=1}^{n}|O_i - E_i|\right) \quad (2)$$

Fit $= R^2$ where R is Pearson's correlation between O_i y E_i.

The values of O_i have been standardised between 0 and 1. The results obtained are depicted in Table 1.

The results show great fits and low errors. Besides, Snedecor's F test to validate the **LinR** model gives a value of F = 23,669, with a probability queue $p < 0.001$. Therefore, there is at least one significant linear functional relationship, and there could be a non-linear relationship because of the good results of SVR-KG. Thus, yes, our proposed RGB_method can replace the reference method.

Table 1
Results of different models to adjust the values of ABS 330.

	MSE	MAE	Adjustment (R^2)
LinR	0.0108585	0.0819458	0.6961003
SVR	0.0135306	0.0868035	0.6771253
SVR-GK	0.0085048	0.0599027	0.7700693

3.7.2. Is the concentration of amino acids in a chronic wound related to its condition?

The state of the chronic wounds was determined by four parameters or pathologies: infectious appearance, bad evolution, necrosis and ischemia. Then, we compared these results with the amino acid concentration obtained by reference method and our proposed RGB_method. For this study, three linear classification methods were used: discriminant analysis (**DA**), logistic regression **(LR**) and support vector machine (**SVM)**. With the observed data, a set of coefficients was determined (c_i) accompanying the explanatory variables, plus a free coefficient c_0. With these coefficients, the classification/diagnosis of a specific case was obtained by calculating the *val* parameter with Eq. 3, where m is the number of explanatory variables and $v_1,\ldots,\ v_m$ are the values of these variables for this case. In this way, if $val > 0$, the case is diagnosed positive (YES) and otherwise negative (NO).

Table 2 depicts the results obtained by the three methods considered, using the absorbance at 330 nm in the case of reference method ($m = 1$), and RGB parameters in the case of the RGB_method ($m = 3$) as explanatory variables for all analysed medical parameters. The results include the number of successes (Sc, i.e. number of correctly diagnosed cases), the ratio (rat, from 0 to 1), and the number of positive and negative cases for each parameter.

$$val = c_0 + c_1\cdot v_1 + \cdots + c_m\cdot v_m \quad (3)$$

For reference method, apparently, there are several combinations parameter/method where an interesting rate of success is reached (in fact 12 of 16 over 68 %). Still, we must be cautious about this: when the cases of each group are unbalanced as in this database, the classification

Table 2
Results obtained by the diagnostic methods (discriminant analysis, **DA**, logistic regression, **LR**, and support vector machine, **SVM**) using both reference method and RGB_method as explanatory variables (absorbance at 330 nm and RGB parameters respectively).

Experimental method	Medical parameter	Cases		Analysis method		
		No	Yes	DA	LR	SVM
Reference method	Infectious aspect	26	9	16 **(Sc)** *0.4571* ***(rat)***	26 *0.7429*	26 *0.7429*
	Bad evolution	21	14	20 *0.5714*	**24** *0.6857*	21 *0.6*
	Necrosis	26	9	24 *0.6857*	25 *0.7143*	26 *0.7429*
	Ischemia	28	7	24 *0.6857*	27 *0.7714*	28 *0.8*
RGB_method	Infectious aspect	25	9	19 *0.5588*	23 *0.6765*	25 *0.7353*
	Bad evolution	21	13	19 *0.5588*	**22** *0.6471*	21 *0.6176*
	Necrosis	25	9	21 *0.6176*	**31** *0.9118*	25 *0.7353*
	Ischemia	27	7	22 *0.6471*	26 *0.7647*	27 *0.7941*

methods can be limited to say that all are from the most numerous group and artificially get a good result. Therefore, initially, we only consider a number of successes higher than the largest group to be interesting. So that the diagnosis of the *bad evolution* explained by **LR** is an interesting result. For the RGB_method, we would consider as exciting the diagnosis of the *bad evolution* defined by LR and especially the 31 successes of 34 cases also achieved with **LR** in the diagnosis of *necrosis*. In short, the concentration of amino acids is directly correlated with the state of the wound, regardless of whether it was obtained using the reference method, or using the RGB_method. Even in the case of *necrosis*, the RGB_method combined with the **LR** method gives exciting results.

3.8. Figure of merits

There are many techniques/methods in the literature for detecting protease activity qualitatively or quantitatively. However, in most cases, these procedures need much time and/or their costs are very high because they require extensive instrumentation. Table 3 shows a short study of the published detection methods for amino acid, in terms of the low-cost character, response time and naked-eye detection.

4. Conclusions

We propose a new method and methodology for the control and diagnosis of chronic wounds based on pictures taken to discs cut from sensory films, which change their colour upon entering into contact with amino acids. The sensory polymeric material is inexpensively prepared by straightforward procedures from 99 % of commercially available monomers. The experimental procedure is simple, neither reactants nor expensive equipment are needed, and can be straightforward carried out by untrained personnel by taking a photograph with a smartphone to the sensory material after immersing in the exudate. The sensor can be used in a broad pH range and has no interference with a vast number of anions and cations. Additionally, we have demonstrated that the state/evolution of the wound correlates with the concentration of amino acids. The chosen reference method for measuring amino acids (Nielsen method) [41] has shown to have good results in wound diagnosis. Mainly, in the case of *bad evolution*, the results are fascinating. In the other hand, it has been established that there is a functional relationship between the values of this reference method and the values of the digital colour of the photograph of the discs (R, G and B parameters). Even, the RGB values show to have a diagnostic capability of chronic wounds similar to the reference method, and better in the case of *necrosis*. We have used linear models, for data treatment and predictions, which are conceptually simple to understand and apply. However, more sophisticated models could significantly improve the quality of the results, and could be integrated into an easy to use software or smartphone app.

Table 3
Comparative table of analytical methods for amino acids.

Method name	Detection method	Low-cost[a]	Response time	Naked eye detection	Refs.
Reference method	UV–vis	no	15min	no	[41]
Spectrophotometric		no	1h	no	[58]
Quenched BODIPY	Fluorescence	no	1.5h	no	[59]
Fluorescence Polarisation		no	2h	no	[60]
SPR sensor		no	30min	no	[61]
Direct measurement		no	3.5h	no	[62]
Densitometry	Scanning densitometry	no	3h	no	[63]
In vivo	Metal-oxide-semiconductor imaging device	no	5h	no	[64]
Free porous silicon (PSi) photonic crystals	Optical Reflectivity	no	24h	no	[65]
Nanopore sensor	potentiometric	no	2h	no	[66]
RGB	Digital pictures (RGB parameters defining the digital colours)	yes	1h	yes	This work

[a] Low-cost: no need of equipment, maintenance and lab space for the equipment, and trained personal to carry on the measurements.

CRediT authorship contribution statement

Marta Guembe-García: Validation, Investigation, Writing - original draft. **Victoria Santaolalla-García:** Conceptualization, Validation, Investigation, Resources. **Natalia Moradillo-Renuncio:** Conceptualization, Validation, Investigation, Resources. **Saturnino Ibeas:** Methodology, Validation, Formal analysis. **Jose A. Reglero:** Validation, Formal analysis, Investigation. **Félix C. García:** Conceptualization, Methodology, Writing - review & editing, Supervision. **Joaquín Pacheco:** Methodology, Validation, Formal analysis, Writing - review & editing. **Silvia Casado:** Methodology, Validation, Formal analysis. **José M. García:** Conceptualization, Methodology, Writing - review & editing, Supervision, Project administration, Funding acquisition. **Saul Vallejos:** Conceptualization, Methodology, Investigation, Writing - original draft, Writing - review & editing, Supervision.

Declaration of Competing Interest

The authors declare that there is no conflict of **interest**.

Acknowledgements

We gratefully acknowledged the financial support provided by Fondo Europeo de Desarrollo Regional and both the Spanish Ministerio de Economía, Industria y Competitividad (MAT2017-84501-R and ECO2016-76567-C4-2-R) and the Consejería de Educación, Junta de Castilla y León (BU306P18 and BU071G19).

Appendix A. Supplementary data

Supplementary material related to this article can be found, in the online version, at doi:https://doi.org/10.1016/j.snb.2021.129688.

References

[1] C.D. Hinman, H. Maibach, Effect of air exposure and occlusion on experimental human skin wounds, Nature 200 (1963) 377–378, https://doi.org/10.1038/200377a0.
[2] G.C. Gurtner, S. Werner, Y. Barrandon, M.T. Longaker, Wound repair and regeneration, Nature. 453 (2008), https://doi.org/10.1038/nature07039.
[3] G.M. Sundaram, J.E.A. Common, F.E. Gopal, S. Srikanta, K. Lakshman, D.P. Lunny, T.C. Lim, V. Tanavde, E.B. Lane, P. Sampath, 'See-saw' expression of microrna-198 and fstl1 from a single transcript in wound healing, Nature 495 (2013) 103–106, https://doi.org/10.1038/nature11890.xperimental metho.
[4] P. Martin, J. Lewis, Actin cables and epidermal movement in embryonic wound healing, Nature 360 (1992) 179–183, https://doi.org/10.1038/360179a0.
[5] M. Zhao, B. Song, J. Pu, T. Wada, B. Reid, G. Tai, F. Wang, A. Guo, P. Walczysko, Y. Gu, T. Sasaki, A. Suzuki, J.V. Forrester, H.R. Bourne, P.N. Devreotes, C. D. McCaig, J.M. Penninger, Electrical signals control wound healing through phosphatidylinositol-3-OH kinase-γ and PTEN, Nature 442 (2006) 457–460, https://doi.org/10.1038/nature04925.
[6] M.C. Coles, C.D. Buckley, Ready-made cellular plugs heal skin wounds, Nature 576 (2019) 215–216, https://doi.org/10.1038/d41586-019-03602-4.
[7] S. Mahmoudi, E. Mancini, L. Xu, A. Moore, F. Jahanbani, K. Hebestreit, R. Srinivasan, X. Li, K. Devarajan, L. Prélot, C.E. Ang, Y. Shibuya, B.A. Benayoun, A.L.S. Chang, M. Wernig, J. Wysocka, M.T. Longaker, M.P. Snyder, A. Brunet, Heterogeneity in old fibroblasts is linked to variability in reprogramming and wound healing, Nature 574 (2019) 553–558, https://doi.org/10.1038/s41586-019-1658-5.
[8] P. Gómez Fernández, Revisión del tratamiento de las úlceras venosas: terapia compresiva, RqR Enfermería Comunitaria. 3 (2015) 43–54.

[9] J. Posnett, F. Gottrup, H. Lundgren, G. Saal, The resource impact of wounds on health-care providers in Europe, J. Wound Care 18 (2009) 154–161, https://doi.org/10.12968/jowc.2009.18.4.41607.

[10] S.R. Nussbaum, M.J. Carter, C.E. Fife, J. DaVanzo, R. Haught, M. Nusgart, D. Cartwright, An economic evaluation of the impact, cost, and medicare policy implications of chronic nonhealing wounds, Value Heal. 21 (2018) 27–32, https://doi.org/10.1016/j.jval.2017.07.007.

[11] L. MacGregor, K. Day, Principles of Best Practice: Diagnostics and Wounds. A Consensus Document, Medical Education Partnership (MEP), London, 2008.

[12] K. Day, Consenso Internacional. Función De Las Proteasas En El Diagnóstico De Heridas. Revisión De Un Grupo De Trabajo De Expertos, Wounds International Enterprise House, London, 2011.

[13] M.J. Westby, J.C. Dumville, N. Stubbs, G. Norman, N. Cullum, Protease-modulating matrix treatments for healing venous leg ulcers, Cochrane Database Syst. Rev. 2015 (2015), https://doi.org/10.1002/14651858.CD011918.

[14] D.E. Kleiner, W.G. Stetlerstevenson, Quantitative zymography: detection of picogram quantities of gelatinases, Anal. Biochem. 218 (1994) 325–329, https://doi.org/10.1006/abio.1994.1186.

[15] Z.S. Calis, G.K. Sukhova, P. Libby, Microscopic localization of active proteases by in situ zymography: detection of matrix metalloproteinase activity in vascular tissue, FASEB J. 9 (1995) 974–980, https://doi.org/10.1096/fasebj.9.10.7615167.

[16] M.F. Clark, A.N. Adams, Characteristics of the microplate method of enzyme linked immunosorbent assay for the detection of plant viruses, J. Gen. Virol. 34 (1977) 475–483, https://doi.org/10.1099/0022-1317-34-3-475.

[17] M.T. Veledo, M. De Frutos, J.C. Diez-Masa, Amino acids determination using capillary electrophoresis with on-capillary derivatization and laser-induced fluorescence detection, J. Chromatogr. A 1079 (2005) 335–343, https://doi.org/10.1016/j.chroma.2005.03.111.

[18] A.E. Pasieka, M.E. Thomas, The detection of β-alanine in biological fluids, Clin. Biochem. 2 (1968) 423–429, https://doi.org/10.1016/s0009-9120(68)80101-8.

[19] K. Mopper, P. Lindroth, Diel and depth variations in dissolved free amino acids and ammonium in the Baltic Sea determined by shipboard HPLC analysis, Limnol. Oceanogr. 27 (1982) 336–347, https://doi.org/10.4319/lo.1982.27.2.0336.

[20] K. Petritis, C. Elfakir, M. Dreux, HPLC-CLND for the analysis of underivatized amino acids, LC GC Eur. 14 (2001) 389–395.

[21] S. Katsikis, I. Marin-Montesinos, C. Ludwig, U.L. Günther, Detecting acetylated aminoacids in blood serum using hyperpolarized 13C-1H-2D-NMR, J. Magn. Reson. 305 (2019) 175–179, https://doi.org/10.1016/j.jmr.2019.07.003.

[22] K. Adriaenssens, R. Vanheule, D. Karcher, Y. Hardens, A simple screening method for the study of amino acids in tissues using frozen slices, Clin. Chim. Acta 18 (1967) 351–354, https://doi.org/10.1016/0009-8981(67)90030-7.

[23] A. Saifer, Rapid screening methods for the detection of inherited and acquired aminoacidopathies, Adv. Clin. Chem. 14 (1971) 145–218, https://doi.org/10.1016/S0065-2423(08)60146-8.

[24] A. Szeinberg, B. Szeinberg, B.E. Cohen, Screening method for detection of specific aminoacidemias, Clin. Chim. Acta 23 (1969) 93–95, https://doi.org/10.1016/0009-8981(69)90015-1.

[25] D. Kumar, M. Abdul Rub, M. Akram, Kabir-Ud-Din, Interaction of chromium(III) complex of glycylphenylalanine with ninhydrin in aqueous and cetyltrimethylammonium bromide (CTAB) micellar media, Tenside, Surfactants, Deterg. 51 (2014) 157–163, https://doi.org/10.3139/113.110296.

[26] C.B. Bottom, S.S. Hanna, D.J. Siehr, Mechanism of the ninhydrin reaction, Biochem. Educ. 6 (1978) 4–5, https://doi.org/10.1016/0307-4412(78)90153-X.

[27] S. Ruhemann, CXXXII. - Cyclic di- and tri-ketones, J. Chem. Soc. Perkin Trans. I 97 (1910) 1438–1449, https://doi.org/10.1039/CT9109701438.

[28] S. Ruhemann, LXXXIV. - triketohydrindene hydrate. Part III. Its relation to alloxan, J. Chem. Soc. Perkin Trans. I 99 (1911) 792–800, https://doi.org/10.1039/CT9119900792.

[29] S. Ruhemann, CXLII. - triketohydrindene hydrate. Part IV. Hydrindantin and its analogues, J. Chem. Soc. Perkin Trans. I 99 (1911) 1306–1310, https://doi.org/10.1039/CT9119901306.

[30] S. Ruhemann, CLXX. - Triketohydrindene hydrate. Part V. The analogues of uramil and purpuric acid, J. Chem. Soc. Perkin Trans. I 99 (1911) 1486–1492, https://doi.org/10.1039/CT9119901486.

[31] M. Friedman, Applications of the ninhydrin reaction for analysis of amino acids, peptides, and proteins to agricultural and biomedical sciences, J. Agric. Food Chem. 52 (2004) 385–406, https://doi.org/10.1021/jf030490p.

[32] D.J. McCaldin, The chemistry of ninhydrin, Chem. Rev. 60 (1960) 39–51, https://doi.org/10.1021/cr60203a004.

[33] J.H. Holtz, S.A. Asher, Polymerized colloidal crystal hydrogel films as intelligent chemical sensing materials, Nature 389 (1997) 829–832, https://doi.org/10.1038/39834.

[34] J. Xiao, Y. Tan, Y. Song, Q. Zheng, A flyweight and superelastic graphene aerogel as a high-capacity adsorbent and highly sensitive pressure sensor, J. Mater. Chem. A Mater. Energy Sustain. 6 (2018) 9074–9080, https://doi.org/10.1039/c7ta11348j.

[35] J. Hou, M. Liu, H. Zhang, Y. Song, X. Jiang, A. Yu, L. Jiang, B. Su, Healable green hydrogen bonded networks for circuit repair, wearable sensor and flexible electronic devices, J. Mater. Chem. A Mater. Energy Sustain. 5 (2017) 13138–13144, https://doi.org/10.1039/c7ta03100a.

[36] H.J. Salavagione, A.M. Díez-Pascual, E. Lázaro, S. Vera, M.A. Gómez-Fatou, Chemical sensors based on polymer composites with carbon nanotubes and graphene: the role of the polymer, J. Mater. Chem. A Mater. Energy Sustain. 2 (2014) 14289–14328, https://doi.org/10.1039/c4ta02159b.

[37] M. Guembe-García, P.D. Peredo-Guzmán, V. Santaolalla-García, N. Moradillo-Renuncio, S. Ibeas, A. Mendía, F.C. García, J.M. García, S. Vallejos, Why is the sensory response of organic probes within a polymer film different in solution and in the solid-state? Evidence and application to the detection of amino acids in human chronic wounds, Polymers (Basel). 12 (2020) 1249, https://doi.org/10.3390/polym12061249.

[38] J.E. Eastoe, The amino acid composition of proteins from the oral tissues-II. The matrix proteins in dentine and enamel from developing human deciduous teeth, Arch. Oral Biol. 8 (1963) 633–652, https://doi.org/10.1016/0003-9969(63)90078-5.

[39] F.W. Keeley, S.M. Partridge, Amino acid composition and calcification of human aortic elastin, Atherosclerosis. 19 (1974) 287–296, https://doi.org/10.1016/0021-9150(74)90063-X.

[40] J.E. Eastoe, P. Martens, N.R. Thomas, The amino-acid composition of human hard tissue collagens in osteogenesis imperfecta and dentinogenesis imperfecta, Calcif. Tissue Res. 12 (1973) 91–100, https://doi.org/10.1007/BF02013724.

[41] P.M. Nielsen, Improved method for determining protein hydrolysis, J. Food Sci. 66 (2001) 642–646.

[42] S. Vallejos, D. Moreno, S. Ibeas, A. Muñoz, F.C. García, J.M. García, Polymeric chemosensor for the colorimetric determination of the total polyphenol index (TPI) in wines, Food Control 106 (2019) 106684, https://doi.org/10.1016/j.foodcont.2019.06.010.

[43] S. Vallejos, E. Hernando, M. Trigo, F.C. García, M. García-Valverde, D. Iturbe, M. J. Cabero, R. Quesada, J.M. García, Polymeric chemosensor for the detection and quantification of chloride in human sweat. Application to the diagnosis of cystic fibrosis, J. Mater. Chem. B Mater. Biol. Med. 6 (2018) 3735–3741, https://doi.org/10.1039/c8tb00682b.

[44] S. Vallejos, A. Muñoz, S. Ibeas, F. Serna, F.C. García, J.M. García, Solid sensory polymer substrates for the quantification of iron in blood, wine and water by a scalable RGB technique, J. Mater. Chem. A Mater. Energy Sustain. 1 (2013) 15435–15441, https://doi.org/10.1039/c3ta12703f.

[45] S. Vallejos, J.A. Reglero, F.C. García, J.M. García, Direct visual detection and quantification of mercury in fresh fish meat using facilely prepared polymeric sensory labels, J. Mater. Chem. A Mater. Energy Sustain. 5 (2017) 13710–13716, https://doi.org/10.1039/c7ta03902f.

[46] S. Vallejos, P. Estévez, S. Ibeas, F.C. García, F. Serna, J.M. García, An organic/inorganic hybrid membrane as a solid "Turn-On" fluorescent chemosensor for coenzyme a (CoA), cysteine (Cys), and glutathione (GSH) in aqueous media, Sensors 12 (2012) 2969–2982, https://doi.org/10.3390/s120302969.

[47] A. Tharwat, Linear vs. Quadratic discriminant analysis classifier: a tutorial, Int. J. Appl. Pattern Recognit. 3 (2016) 145, https://doi.org/10.1504/ijapr.2016.079050.

[48] I.L. Lottes, M.A. Adler, A. DeMaris, Using and interpreting logistic regression: a guide for teachers and students, Teach. Sociol. 24 (1996) 284–298, https://doi.org/10.2307/1318743.

[49] V. Vapnik, The support vector method of function estimation. Nonlinear Model, Springer, US, 1998, pp. 55–85, https://doi.org/10.1007/978-1-4615-5703-6_3.

[50] G. Rozenberg, T. Back, J.N. Kok, Handbook of Natural Computing, 2012, https://doi.org/10.1007/978-3-540-92910-9.

[51] H. Yu, S. Kim, SVM tutorial-classification, regression and ranking, Handb. Nat. Comput. 1–4 (2012) 479–506, https://doi.org/10.1007/978-3-540-92910-9_15.

[52] S. Vallejos, E. Hernando, M. Trigo, F.C. García, M. García-Valverde, D. Iturbe, M. J. Cabero, R. Quesada, J.M. García, Polymeric chemosensor for the detection and quantification of chloride in human sweat. Application to the diagnosis of cystic fibrosis, J. Mater. Chem. B Mater. Biol. Med. 6 (2018) 3735–3741, https://doi.org/10.1039/c8tb00682b.

[53] S.E. Bustamante, S. Vallejos, B.S. Pascual-Portal, A. Muñoz, A. Mendia, B.L. Rivas, F.C. García, J.M. García, Polymer films containing chemically anchored diazonium salts with long-term stability as colorimetric sensors, J. Hazard. Mater. 365 (2019) 725–732, https://doi.org/10.1016/j.jhazmat.2018.11.066.

[54] M.M. Joullié, T.R. Thompson, N.H. Nemeroff, Ninhydrin and ninhydrin analogs. Syntheses and applications, Tetrahedron 47 (1991) 8791–8830, https://doi.org/10.1016/S0040-4020(01)80997-2.

[55] M. Yin, Y. Ye, M. Sun, N. Kang, W. Yang, Facile one-pot synthesis of a polyvinylpyrrolidone-based self-crosslinked fluorescent film, Macromol. Rapid Commun. 34 (2013) 616–620, https://doi.org/10.1002/marc.201200750.

[56] D.C. Wigfield, G.W. Buchanan, S.M. Croteau, On Ruhemann's purple, Can. J. Chem. 58 (1980) 201–205, https://doi.org/10.1139/v80-032.

[57] M. Guembe-García, P.D. Peredo-Guzmán, V. Santaolalla-García, N. Moradillo-Renuncio, S. Ibeas, A. Mendía, F.C. García, J.M. García, S. Vallejos, Why the sensory response of organic probes is different in solution and in the solid- state within a polymer film? Evidence and application to the detection of amino acids in human chronic wounds, Polymers 12 (2020) 1249.

[58] S. Stephan, H. Schwarz, A. Borchert, D. Bussfeld, E. Quak, B. Simshaeuser-Knaub, S. Teigelkamp, F. Behrens, F. Vitzthum, Tests for the measurement of factor VII-activating protease (FSAP) activity and antigen levels in citrated plasma, their correlation to PCR testing, and utility for the detection of the Marburg I-polymorphism of FSAP, Clin. Chem. Lab. Med. 46 (2008) 1109–1116, https://doi.org/10.1515/CCLM.2008.218.

[59] L.J. Jones, R.H. Upson, R.P. Haugland, N. Panchuk-Voloshina, M. Zhou, R. P. Haugland, Quenched BODIPY dye-labeled casein substrates for the assay of protease activity by direct fluorescence measurement, Anal. Biochem. 251 (1997) 144–152, https://doi.org/10.1006/abio.1997.2259.

[60] L.M. Levine, M.L. Michener, M.V. Toth, B.C. Holwerda, Measurement of specific protease activity utilizing fluorescence polarization, Anal. Biochem. 247 (1997) 83–88, https://doi.org/10.1006/abio.1997.2047.

[61] J. Park, G. Baik Kim, A. Lippitz, Y.M. Kim, D. Jung, W.E.S. Unger, Y.P. Kim, T. G. Lee, Plasma-polymerized antifouling biochips for label-free measurement of

protease activity in cell culture media, Sensors Actuators, B Chem. 281 (2019) 527–534, https://doi.org/10.1016/j.snb.2018.10.123.
[62] N. Safa, J.H. Pettigrew, T.J. Gauthier, A.T. Melvin, Direct measurement of deubiquitinating enzyme activity in intact cells using a protease-resistant, cell-permeable, peptide-based reporter, Biochem. Eng. J. 151 (2019) 107320, https://doi.org/10.1016/j.bej.2019.107320.
[63] Y. Mori, H. Wada, E.C. Gabazza, N. Minami, T. Nobori, H. Shiku, H. Yagi, H. Ishizashi, M. Matsumoto, Y. Fujimura, Predicting response to plasma exchange in patients with thrombotic thrombocytopenic purpura with measurement of vWF-cleaving protease activity, Transfusion 42 (2002) 572–580, https://doi.org/10.1046/j.1537-2995.2002.00100.x.
[64] D.C. Ng, H. Tamura, T. Tokuda, A. Yamamoto, M. Matsuo, M. Nunoshita, Y. Ishikawa, S. Shiosaka, J. Ohta, Real time in vivo imaging and measurement of serine protease activity in the mouse hippocampus using a dedicated complementary metal-oxide semiconductor imaging device, J. Neurosci. Methods 156 (2006) 23–30, https://doi.org/10.1016/j.jneumeth.2006.02.005.
[65] B. Gupta, K. Mai, S.B. Lowe, D. Wakefield, N. Di Girolamo, K. Gaus, P.J. Reece, J. J. Gooding, Ultrasensitive and specific measurement of protease activity using functionalized photonic crystals, Anal. Chem. 87 (2015) 9946–9953, https://doi.org/10.1021/acs.analchem.5b02529.
[66] L. Wang, Y. Han, S. Zhou, X. Guan, Real-time label-free measurement of HIV-1 protease activity by nanopore analysis, Biosens. Bioelectron. 62 (2014) 158–162, https://doi.org/10.1016/j.bios.2014.06.041.

Marta Guembe-García received her Master's degree in biomedical physics at the Complutense University of Madrid, Spain, in 2017. Now she is a researcher staff at the Department of Chemistry, University of Burgos and she is doing her PhD studies in Advanced Chemistry since 2018. Her research interests include polymer sensors with biomedical applications.

Victoria Santaolalla-García received her degree in Medicine and Surgery at the Cantabrian University in 2006 and finished her specialty in Angiology and Vascular Surgery at University Hospital of Burgos in 2012. She is doing her PhD studies in Frailty as a marker in patients with critical limb ischaemia since 2017. She holds a Diabetic Foot Expert Qualification and ETV-Cancer Master. Her research interests include infection, would healing and proteases role in the process.

Natalia Moradillo-Renuncio received her degree in Medicine and Surgery at the Valladolid University in 2010 and finished her specialty in Angiology and Vascular Surgery at University Hospital of Burgos in 2016. She holds a Diabetic Foot Expert Qualification and ETV-Cancer Master. She is doing a degree in biostatistics at Barcelona University since 2019. Her research interests include inflammatory biomarkers in wound healing.

Saturnino Ibeas is Professor at the Department of Chemistry at the University of Burgos, Spain. He carried out his doctoral studies at the Department of Physical Chemistry at the University of Valladolid, receiving his Ph.D. in Chemistry at the University of Valladolid, Spain in 1994. Prof. Ibeas is a co-author of more than 30 peer reviewed scientific publications. His principal areas of research are study of DNA-ligand interaction and thermodynamic and kinetic study of the complexation reactions.

José Antonio Reglero obtained his PhD in Physics in 2007 from the University of Valladolid (SPAIN), with a work focused in the fabrication and characterization of aluminium foams. His research career has been developed in different laboratories of Spain (Cellmat) and France (LCPO, ICMCB and CEMEF), working in the fabrication, characterization and analysis of properties of cellular polymers. Since 2016, he joined the Polymer Research Group at the University of Burgos, in which he is currently working on the synthesis, characterization and applications of sensory polymers. He has published 41 research works, and given 15 invited talks in international conferences and two book chapters.

Félix Clemente García is Professor of the Department of Chemistry at the University of Burgos, Spain. He received his PhD at the University of Burgos, Spain in 2001. His research interest is in polymers with sensing capabilities in water environments.

Joaquín Pacheco is Full Professor at the University of Burgos since 2009. He teaches Mathematics, Statistics and Operations Research at the Faculty of Economics and Business. He received his PhD in Mathematics (Operations Research) from the Complutense University of Madrid in 1994. The lines of research are focused on the design of metaheuristic methods, multi-objective optimization and data mining. He has published more than 40 articles in JCR journals (20 Q1). He has been principal investigator in several competitive, regional and national projects, as well as in contracts with public and private entities.

Silvia Casado is currently Associate Professor in Mathematics and Operations Research at the University of Burgos, Spain. She received her Ph.D. in Business (Operations Research) from the University of Burgos in 2003. The field of applications of his research includes social applications such as school transport, urban transport, location of medical facilities, classification methods applied to diagnosis of diseases, etc. She has published about 25 publications indexes by JCR and SJR. She has joined in different competitive National Projects supported by public entities such as Spanish Ministry of Education and Science, Ministry of Science and Innovation, Ministry of Economy and Competitiveness and Regional government of Castilla and León.

José Miguel García is Full Professor at the Department of Chemistry at the University of Burgos, Spain. He carried out his doctoral studies at the Institute of Polymer Science & Technology, Spanish National Research Council (CSIC), receiving his PhD in Chemistry at the Complutense University of Madrid, Spain in 1995. Prof. Garcia is a co-author of 110+ peer reviewed scientific publications and has a number of patents, along with co-author books and books chapters. His principal areas of research are high performance materials, functional polymers, and sensory polymers as sensing materials for food, biomedical, environmental, and civil security applications.

Saúl Vallejos received his PhD in Chemistry in 2014 from the University of Burgos, Spain. Now he is a postdoc researcher at the Department of Chemistry, University of Burgos. His research interests are functional polymers having receptor motifs as sensory materials toward anions, cations, and neutral molecules.